Non-Isolated Single-Inductor DC/DC Converter with Fully Reconfigurable Structure for Renewable Energy Applications

Tian Cheng, *Student Member, IEEE*, Dylan Dah-Chuan Lu, *Senior Member, IEEE* and Ling Qin

***Abstract*—A novel non-isolated three-port converter (NITPC) is introduced in this brief. The purpose of this topology is to integrate a regenerative load such as DC bus and motor with dynamic braking, instead of the widely reported consuming load, with a photovoltaic (PV)-battery system. Conventional methods require either a separate dc-dc converter to process the reversible power flow or employing an isolated three-port converter (TPC) which allows bi-directional power flow between any two ports. However, these methods require many switches which increases the converter size and control complexity. This brief hence presents a compact but fully functional design by combining and integrating basic converters to form a simplified single-inductor converter structure while keeping minimum amount of switches. The resultant converter is fully reconfigurable that all possible power flow combinations among the sources and load are achieved through different switching patterns, while preserving the single power processing feature of TPC. This brief presents a design example of the proposed NITPC for a PV-battery powered DC microgrid. Detailed circuitry analysis, operation principles of both DC grid-connected and islanded modes, and experimental results of different modes in steady state and mode transitions are presented.**

***Index Terms*—Three-port converter, DC microgrids, single-inductor, renewable energy, energy storage.**

I. Introduction

RECENTLY, three-port converters are gaining popularity among applications which integrate renewable energies and energy storage with the load (e.g. satellite system, hybrid vehicle, etc.). A number of three-port converter (TPC) topologies have been proposed for the benefits of single-stage power conversion between any two ports. The formation of non-isolated TPCs (NITPCs) is based on a generic multiple-input multiple-output structure [1]-[3]. In [4], the authors reviewed and compared recently published non-isolated, partly-isolated and isolated TPCs. NITPCs are cost-effective and are compact due to the reduced components. Their control strategy are simple as NITPCs are derived from basic converters [2]-[3]. However, for the same reason, the voltage gain of NITPC is limited. Partly-isolated TPCs can provide a high voltage gain and isolation between two ports. However, they have limited power flow options due to partially shared devices. Isolated TPCs can achieve high voltage gain, high power operation and provide galvanic isolation while offering single-stage power conversion between any two ports. However, the three-winding transformer and many switches increases the converter size and cost. Overall, most of the reviewed TPCs in [4] are designed for power consuming loads, as shown in Fig. 1(a).

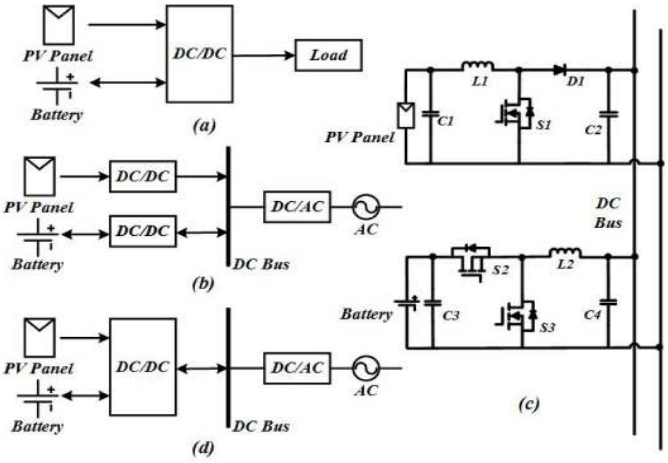

Fig. 1: (a) Three-port converter for stand-alone system. (b) DC microgrids with two independent converters. (c) A topology example of (b). (d) Isolated TPC and proposed NITPC structure for DC microgrids.

However, there also exist some loads with power generating capability such as dynamic braking in electric vehicles and DC microgrids. Most common solutions to interfacing with a regenerative load can be divided into two groups. One is to use an extra bi-directional converter between the battery and the DC bus as shown in Fig. 1(b). A topology example of this solution is shown in Fig. 1(c), which is derived and developed from [5]. In [6], a soft-switched non-isolated bi-directional converter is proposed for the battery to interface with the DC microgrid with a high voltage gain and reduced switch numbers. However, this converter structure requires a two-stage power conversion when the PV panel charges the battery,

Manuscript received February 21, 2017; revised April 21, 2017; accepted May 5, 2017. Date of publication June 6, 2017; date of current version March 8, 2018. This brief was recommended by Associate Editor H.-J. Chiu. (Corresponding author: Tian Cheng.)

T. Cheng is with The University of Sydney, NSW 2006, Australia (e-mail: tche2451@uni.sydney.edu.au).

D. D.-C. Lu is with the School of Electrical and Data Engineering, University of Technology Sydney, NSW 2007, Australia, and also with The University of Sydney, NSW 2006, Australia.

L. Qin is with Nantong University, Nantong 226019, China.

which increases power loss due to repeated power processing. Isolated TPCs using the structure in Fig. 1(d) can fulfill bi-directional power flow purposes [4] at the expenses of circuitry and control complexity. In [7], a virtual control scheme is proposed for a triple-independent full-bridge converter employing TPC to prevent the power flowing to an idling port when the other two ports are active (e.g. electric vehicles charges the battery only without powering other loads, etc).

To maintain a single-stage power conversion of the TPC while providing a simple and compact structure for interfacing with a bi-directional load, particularly for low power applications, a NITPC is proposed with the following features:

1) It integrates and controls a current reversible load, hence, it can be applied in wider practical applications.
2) Only one inductor is used, the converter size and cost are reduced while the power density is further improved.
3) Single-stage power conversion between any two ports, which is a key feature in TPCs, is preserved.
4) Since in each mode the TPC reconfigures to basic buck converter and boost converter operations, the control strategies are simple and straightforward.
5) It can be flexibly reconfigured into single-input single-output (SISO), dual-input single-output (DISO) and single-input dual-output (SIDO) modes, to fulfil all possible power flow combinations among the three ports.

II. Circuit Configuration

The proposed NITPC as shown in Fig. 2 is explained in the context of a DC microgrid. The three ports are denoted by voltage sources V_{pv}, V_b and V_{dc} respectively. Among them, the PV panel is the input and is the only unidirectional port, whereas, the other two are bi-directional ports. The DC bus is a current reversible port and is also the main power consumed load whilst the battery port is responsible for balancing the power among the three ports. To have proper converter operation, the three ports are required to follow the voltage settings i.e. $V_{pv} < V_{dc} < V_b$. This topology can be regarded as an integrated boost-buck converter. Inductor L_1 is an essential energy storage element for the input to either step up or down its voltage to the desired output voltage. S_1, S_2, S_3 and S_4 are power switches where MOSFETs are used. S_1 is employed as the main switch of the boost converter for inductor to store energy as well as to realize maximum power point tracking (MPPT) of the PV panel. S_2 is mainly used to control the current flow to the DC bus. S_3 allows the battery to discharge and S_4 allows the DC bus to be an input source. Diode D_1 is used to block current from DC bus or battery from flowing back to the PV panel. Diodes D_2 and D_3 are the output rectifiers of the boost converter for the DC bus and battery respectively. Diode D_2 also disables the body diode of S_2 to allow uni-directional current flow on that branch. D_4 is the free-wheeling diode to provide buck converter operation. D_5 is employed to block the battery current flowing through body diode of S_4 back to DC bus. C_1, C_2 and C_3 are the filter capacitors at PV cells, battery and DC bus respectively. The duty cycles are determined as d_1, d_2, d_3, d_4 and d_5, which are the control variables of S_1, S_2, S_3, S_4 and D_3 respectively.

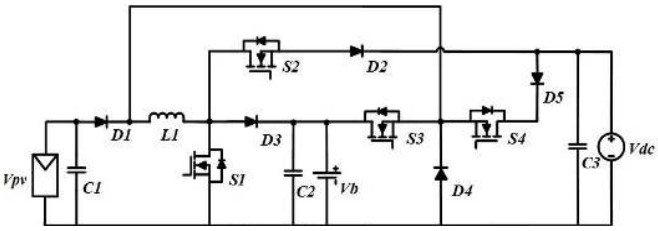

Fig. 2: Proposed converter topology.

III. Circuit Operation Principle

As the proposed NITPC has two bi-directional ports, namely, the battery port and the DC bus port, it increases the combinations of different power flow patterns among the three ports. Overall, the proposed converter is capable of operating in seven different modes based on the power conditions of each port coupled with the battery voltage level which is used to evaluate its state of charge. In DC microgrid application, the aforementioned seven operation modes can be split into grid-connected mode and islanded mode. In grid-connected mode, the DC bus is treated as a current reversible load, which can either absorb or supply power. Modes 1 to 5 belong to this group. Islanded mode occurs when the DC bus is off-grid due to scenarios such as fault in distribution system and regular maintenance. The DC bus therefore connects only with the local consuming loads. Modes 6 and 7 belong to this group. Fig. 3(a) indicates the current representations of each component in this converter. Fig. 3(b) summaries the possible combinations of operation modes among the three ports and the reconfigurable converter types, which can be represented by four SISO converters in black lines, one SIDO converter in blue lines and two DISO converters in red lines.

1) Mode 1 (PV to Battery; Fig. 3(c)): This mode is designed for grid-connected mode where the DC bus is regulated by the AC grid while the PV has just sufficient power to charge the battery. Therefore the converter works like a conventional SISO boost converter. When S_1 turns on, PV stores energy in inductor L_1. When S_1 turns off, D_3 conducts and both PV and L_1 release their energy to battery.

2) Mode 2 (PV to DC bus; Fig. 3(d)): The converter operates in this mode when the battery is fully charged and PV power is available. Hence, PV delivers its energy to DC bus only. The converter operates as a SISO boost converter. S_1 and D_2 work in a complementary manner, and S_1 is used to implement the MPPT. To reduce switching loss, S_2 is turned on for the whole operation mode. D_5 will not conduct since the body diode of S_4 is reverse biased.

3) Mode 3 (PV to battery and DC bus; Fig. 3(e)): This mode happens when PV current is higher than the rated charging current of the battery. Hence, the configuration works as a SIDO boost converter. Due to energy conservation, the PV power equals the sum of the battery power and DC bus power. When S_1 turns on, L_1 is charged. When S_1 turns off, S_2, D_2 and D_3 provide two current paths to dispatch power to DC bus and battery respectively. Eqn.(1) indicates the current ratio of the two outputs, in which d_2 is controlled by S_2 and is determined by the load demand. The remaining current flows

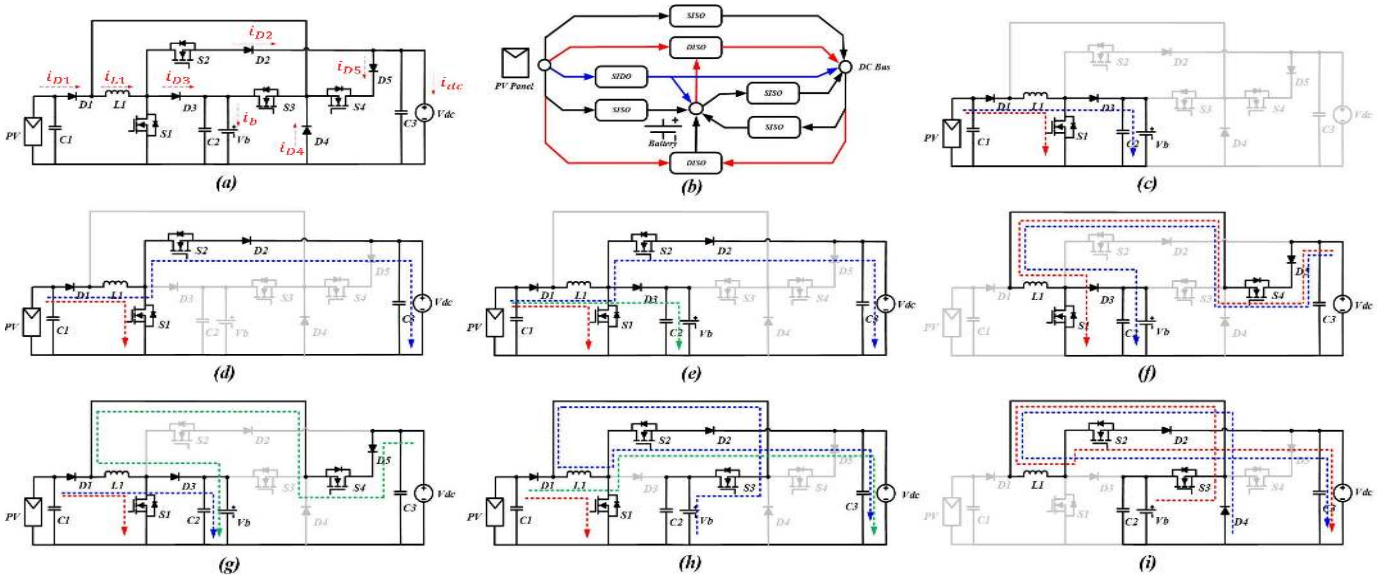

Fig. 3: (a) Topology with current representatives. (b) All possible power conversions among the three ports. Each block (i.e. SISO, SIDO, and DISO) denotes the power flow for which the corresponding power conversion is taken place. (c) Mode 1 (PV to battery). (d) Mode 2 (PV to DC bus). (e) Mode 3 (PV to battery, DC bus). (f) Mode 4 (DC bus to battery). (g) Mode 5 (PV and DC bus to battery). (h) Mode 6 (PV and battery to DC bus). (i) Mode 7 (Battery to DC bus).

to battery regardless of the amount when it is not in full SOC. However, if the battery approaches full SOC, the amount of the charging current needs to be limited. As d_5 is uncontrollable, the control of this current can be realized through controlling S_2 by using the currents relationship in (1).

$$\frac{I_{dc}}{I_b} = \frac{d_2}{d_5} \tag{1}$$

4) Mode 4 (DC bus to battery; Fig. 3(f)): This mode is set to prevent the battery from over-discharging or to store some energy for backup when there is no PV power. Hence, the DC bus needs to charge the battery. The same SISO boost converter in Mode 1 is used but with extra switch S_4 and diode D_5 added to the operation. S_4 fully turns on to allow DC bus to deliver power and to minimize switching loss. Switch S_1 turns on first to charge L_1. When S_1 is off, the power from DC bus and L_1 will be released through diode D_3 to the battery. D_1 is reverse biased, hence, no power flows to PV.

5) Mode 5 (PV and DC bus to battery; Fig. 3(g)): In this mode, to meet the battery charging demand, PV and DC bus work simultaneously. Hence, the converter operates as a DISO converter. The operation includes three periods. Firstly, S_1 turns on to store energy in L_1 from the PV. Secondly, S_1 turns off and S_4 turns on, the DC bus releases power to L_1 and battery. Thirdly, both S_1 and S_4 are off, PV and L_1 deliver energy to battery.

6) Mode 6 (PV and battery to DC bus; Fig. 3(h)): This mode happens when the solar irradiation is insufficient to supply DC bus alone. The battery needs to feed the DC bus simultaneously when DC bus is off-grid. Hence this mode requires a DISO converter structure. There are two switching sequences in this mode depending on the amount of PV power available. In Mode 6A, the PV MPPT function is enabled by turning on S_1. PV charges inductor L_1 first. When S_1 turns off, L_1 is discharged together with battery and PV respectively. In Mode 6B, the MPPT function is disabled, as the PV power decreases and the system intends to switch to Mode 7 where battery alone powers the DC bus. However, since there is a small amount of PV power, the converter turns on S_3 first to let battery charge L_1 and power DC bus. After S_3 is turned off, PV then takes turn to couple energy to L_1 for DC bus.

7) Mode 7 (Battery to DC bus; Fig. 3(i)): This mode happens when there is an absence of PV power whilst DC bus requires power (e.g. night time) in islanded mode. Battery powers the load alone and the converter operates as a SISO buck converter. When S_3 turns on, L_1 is charged. The free wheeling diode D_4 conducts when the S_3 is off. Switch S_2 always turns on in this mode. Similar to Mode 6, d_3 is responsible for regulating the DC bus voltage.

The mode selection criteria and duty cycle of each power switch are summarized in Table I. V_{max} and V_{min} refer to the maximum and minimum preset values to prevent battery from over-charging or discharging. A comparison between the proposed NITPC and conventional two-stage design (Fig. 1(c)) is given in Table I. Some assumptions are made: 1) As most of the PV panels have inner blocking diodes, the loss of D_1 is not considered. 2) In Fig 1.(c), the conversion efficiencies of the boost and buck/boost converters are η_1 and η_2 respectively with $\eta_1 = \eta_2 = 90\%$. 3) The proposed converter and the converter in Fig. 1(c) use the same components. 4) Equal power sharing for DISO and SIDO structures. In Mode 3, a indicates the percentage of P_{pv} transferred to the battery. Based on the assumptions above, the efficiencies of the two converters are estimated. The calculation considers η_1 and η_2 and the extra diodes P_{Dn} and MOSFETs P_{Sn} conduction and switching losses. n indicates the number of switch or diode. The voltage of each port is $V_{pv} = 17\text{V}, V_b =$

TABLE I: Operation Modes Selection and Switches Operation Lookup Table for Each Operation Mode and Comparison with Fig 1.(c)

Modes	*Power* (W)	$V_b(V)$	S_1	S_2	S_3	S_4	*Fig*1.(c) *Active Components*	*Proposed Active Components*
Mode 1	$P_{pv} = P_b$	$V_b < V_{max}$	PWM	0	0	0	$2L + 2S + 2D$	$1L + 1S + 1D$
Mode 2	$P_{pv} = P_{dc}$	$V_b \geq V_{max}$	PWM	1	0	0	$1L + 1S + 1D$	$1L + 2S + 1D$
Mode 3	$P_{pv} = P_{dc} + P_b$	$V_b < V_{max}$	$PWM1$	$PWM2$	0	0	$2L + 2S + 2D$	$1L + 2S + 2D$
Mode 4	$P_{dc} = P_b$	$V_b < V_{max}$	PWM	0	0	1	$1L + 1S + 1D$	$1L + 2S + 2D$
Mode 5	$P_b = P_{pv} + P_{dc}$	$V_b < V_{max}$	PWM	0	0	S_1	$2L + 2S + 2D$	$1L + 2S + 2D$
Mode 6	$P_{pv} + P_b = P_{dc}$	$V_b > V_{min}$	$PWM1$	1	$PWM2$	0	$2L + 2S + 2D$	$1L + 3S + 1D$
			0	1	PWM	0	$2L + 2S + 2D$	$1L + 2S + 1D$
Mode 7	$P_b = P_{dc}$	$V_b > V_{min}$	0	1	PWM	0	$1L + 1S + 1D$	$1L + 2S + 2D$
Modes		*Fig*1.(c) *out −put Power*	*Proposed NITPC output Power*		*Fig*.1(c) $\eta_{1,2} = 90\%$ 50W	500W	*Proposed NITPC* $\eta_{1,2} = 90\%$ 50W	500W
Mode 1 *PV to battery*		$P_{pv} \cdot \eta_1 \cdot \eta_2$	$P_{pv} \cdot \eta_1$		81%	81%	90%	90%
Mode 2 *PV to DC bus*		$P_{pv} \cdot \eta_1$	$P_{pv} \cdot \eta_1 - P_{S2}$		90%	90%	89.9%	89.6%
Mode 3 *PV to battery and DC bus*		$a \cdot P_{pv} \cdot \eta_1 \cdot \eta_2 +$ $(1-a) \cdot P_{pv} \cdot \eta_1$	$a \cdot P_{pv} \cdot \eta_1 - P_{S2} +$ $(1-a) \cdot P_{pv} \cdot \eta_1 - P_{D2}$		85.5%	85.5%	89.9%	89.9%
Mode 4 *DC bus to battery*		$P_{dc} \cdot \eta_2$	$P_{dc} \cdot \eta_2 - P_{D5} - P_{S4}$		90%	90%	87.8%	85%
Mode 5 *PV and DC bus to battery*		$P_{pv} \cdot \eta_1 \cdot \eta_2 +$ $P_{dc} \cdot \eta_2$	$P_{pv} \cdot \eta_1 + P_{dc} -$ $P_{S4} - P_{D5} - P_{D3}$		85.5%	85.5%	93%	92%
Mode 6 *PV and battery to DC bus*		$P_{pv} \cdot \eta_1 +$ $P_b \cdot \eta_2$	$P_{pv} \cdot \eta_1 + P_b -$ $P_{S3} - P_{S2} - P_{D2}$		90%	90%	92%	90%
Mode 7 *battery to DC bus*		$P_b \cdot \eta_2$	$P_b \cdot \eta_2 - P_{D2} - P_{S2}$		90%	90%	87.8%	85%

36V, V_{dc} = 24V. MOSFETs – IRFP4110PbF and Diodes – PMEG6030EVP(3A) and STTH3002G(30A) are used to calculate the efficiencies at 50W and 500W respectively. The results show that the proposed NITPC has a higher overall efficiency than the topology Fig 1.(c) in most of the modes, due to the single-stage power processing. However, it has a lower efficiency in some SISO configurations, mainly due to the additional diode conduction loss.

IV. Experimental Verifications

A downsized hardware prototype is built and tested. However, it is possible to scale up the system by stacking more PV panels and batteries. As the main focus of this paper is to verify the flexible power flow among the three ports, we use a DC source in series with a 5.5Ω resistor to emulate the PV panel (17V). Two battery (DiaMec DM12V-7.2A) tanks are used to implement the storage element (36V) and the DC bus (24V) respectively. Since the battery voltage is related closely with its SOC [8], the battery voltage is used to evaluate the battery capacity for the sake of simplicity. The drivers for PWM of the MOSFETs (IRF540N) are generated by analog circuits while the monitoring and operation mode selection are implemented by the microcontroller (TMS320f28035). The feedback loop is formed by the following process. Firstly, the MCU senses the present voltages and currents of the three ports. Secondly, it determines the operation mode through the following steps: 1) DC bus in grid-connected or islanded mode. 2) Availability of PV power. 3) Battery states, which therefore enables or disables certain switches and sets the references for the analog circuits. Lastly, the analog circuits coupled with the MCU signals generate PWM signals to drive the four MOSFETs. The loop then repeats. The switching frequency is 20kHz, the inductor L_1 is $170uH$, and capacitor C_1, C_2 and C_3 are $100uF$. The measured efficiencies of the experimental setup have shown a similar trend as predicted, with measured efficiencies at 88% and 93% in Modes 4 and 5 respectively at 50W.

A. Vefication of the Operation Modes

Among the seven possible operation modes, four are either basic SISO buck or boost converters, hence only the experimental results of the SIDO and DISO converters are given.

Waveforms of SIDO converter in Mode 2 (PV to battery and DC bus), is shown in Fig. 4(a). As can be observed, the inductor discharging slope is no longer linear, two slope rates are adopted due to the different output voltage levels. i_{D2} or i_{D3} indicate the alternation of power dispatch to the two loads during one switching period.

As both Mode 5 (PV and battery to DC bus) and Mode 6A (PV and DC bus to battery) are DISO converters, and they work in similar manner, only waveforms of Mode 6A are provided as illustrated in Fig. 4(b). d_1 and d_3 represent the duty cycles of switches S_1 and S_3 respectively while i_{D1} and i_{D2} indicate the PV current and diode D_2 current respectively. As can be seen, when S_1 is on, i_{D1} increases. Inductor L_1 is charged while D_2 is reverse biased. When S_3 is on, PV does not supply any power as D_1 is reverse biased. The battery charges both L_1 and DC bus, as the L_1 current keeps on increasing and D_2 is conducting. When both S_1 and S_3 are off, PV and L_1 release their energy to DC bus as D_1 is conducted and inductor current is decreasing. The waveforms of Mode 6B can be observed in Fig. 5(c).

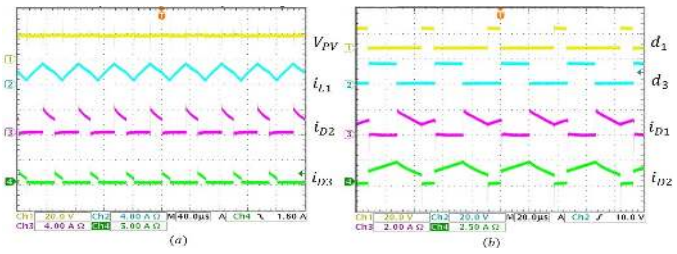

Fig. 4: (a) Mode 3 (PV to battery, DC bus). (b) Mode 6A (PV and battery to DC bus).

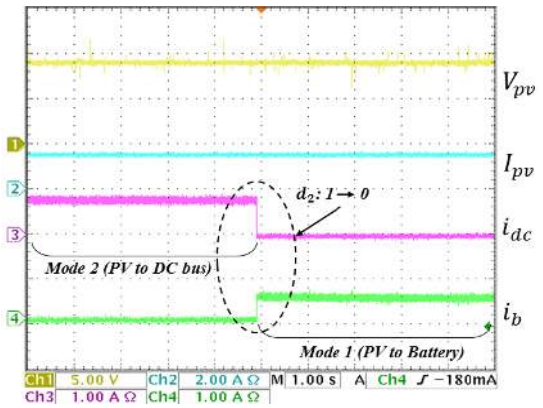

(a) Load switching for PV (Mode 2 to Mode 1).

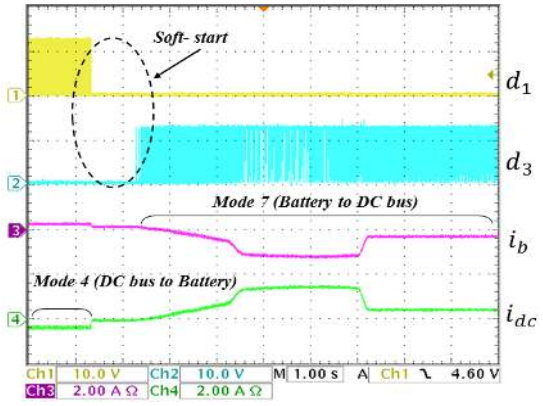

(b) DC bus charges Battery with the bus sudden starts to require power (Mode 4 to Mode 7).

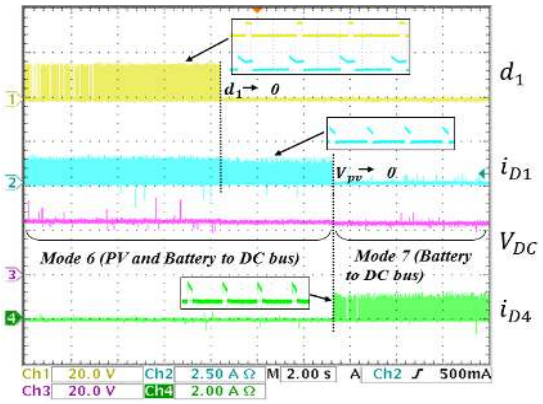

(c) PV and battery charge DC bus then PV stops to supply power (Mode 6 to Mode 7).

Fig. 5: Transition waveforms of shifting the operation modes.

B. Vefication of the Operation Modes Switching

The current and voltage changes in the converter are illustrated to show the transition of the operation modes, as shown in Fig. 5. Three practical scenarios are given as examples:

1) Load switching for PV (Mode 2 to Mode 1): Fig. 5(a) shows the change in consuming loads and the input PV power remains unchanged. This scenario happens when the PV power is limited (e.g. at dusk) to supply the DC bus while the battery is not in full SOC (e.g. battery self-discharge). It will therefore dispatch power to the battery. As can be seen, V_{pv} and i_{pv} are preserved whilst i_{dc} and i_b indicate the current flow switches from DC bus to battery. Moreover, the change between these two modes can be easily achieved by switching S_2.

2) DC bus charges Battery with the bus sudden starts to require power (Mode 4 to Mode 7): This scenario happens when the DC microgrid changes from grid-connected mode to islanded mode, for instance power cut at night time. In order to verify the practicability of the bi-directional operations between the two ports, the transient response is shown in Fig. 5(b). Duty cycles d_1 and d_3 set the on-time for switches S_1 and S_3 respectively. This indicates a change of operation from Mode 4 to Mode 7. The battery current i_b and the DC bus current i_{dc} show the opposite current directions when toggled between the two modes. During transition, the gap between the two pulses is caused by a soft-start function to prevent a large overshoot, and i_b and i_{dc} gradually decrease to zero.

3) PV and battery charge DC bus then PV stops to supply power (Mode 6 to Mode 7): Fig. 5(c) shown the islanded modes switching, and it considers case that solar irradiation decreases to zero and battery needs to supply the load alone. The converter reconfigures from a DISO converter to a SISO buck converter. In Mode 6A, S_1 is in operation for MPPT, while in Mode 6B, it is idled when V_{pv} decreases to the preset value. PV supplies power with battery until it decreases to zero. After PV reaches to zero, the operation switches to Mode 7. i_{D4} represents the current of the free-wheeling diode D_4, showing the buck converter in action. V_{dc} remains constant during the mode switching because in islanded mode, the critical control objective is to maintain the DC bus voltage.

V. Conclusion

A novel single-inductor NITPC is proposed for a PV-battery-DC microgrid. A more flexible power flow can be achieved as two of the three ports are capable of handling reversible currents as compared to one bi-directional port in existing NITPCs. Moreover, a more compact design is realized without using the transformers and full-bridge converters in isolated TPCs which are the common solutions to integrate a bi-directional load. The proposed NITPC can work and transit smoothly between DC grid-connected mode and islanded mode. Detailed operation principles, modes selection requirements and control strategies are explained. The converter can be reconfigured as SISO, SIDO or DISO converter according to the selected mode. A comparison of the proposed NITPC with two separate converters is given. Experimental results are given and verified the flexible operation of the converter.

References

[1] D. Kwon and G. A. Rincon-Mora, "Single-Inductor-Multiple-Output Switching DC-DC Converters," *IEEE Transactions on Circuits and Systems II: Express Briefs.*, 56(8): 614-618, 2009.

[2] Y. J. Moon, Y. S. Roh, J. C. Gong and C. Yoo, "Load-Independent Current Control Technique of a Single-Inductor Multiple-Output Switching DCDC converter," *IEEE Transactions on Circuits and Systems II: Express Briefs.*, 59(1): 50-54, 2012.

[3] K. S. Seol, Y. J. Woo, G. H. Cho, G. H. Gho and J. W. Lee, "A Synchronous Multioutput Step-Up/Down DCDC Converter With Return Current Control," *IEEE Transactions on Circuits and Systems II: Express Briefs.*, 56(3): 210-214, 2009.

[4] N. Zhang, D. Sutanto and K. M. Muttaqi, "A review of topologies of three-port DC/DC converters for the integration of renewable energy and energy storage system." *Renewable and Sustainable Energy Reviews.*, 56 : 388-401, 2016.
[5] X. Xiong, C. K. Tse and X. Ruan, "Bifurcation Analysis of Standalone Photovoltaic-Battery Hybrid Power System." *IEEE Transactions on Circuits and Systems I: Regular Papers.*, 60(5):1354-1365, 2013.
[6] M. Aamir, S. Mekhilef and H. J. Kim, "High-Gain Zero-Voltage Switching Bidirectional Converter With a Reduced Number of Switches," *IEEE Transactions on Circuits and Systems II: Express Briefs.*, 62(8):816-820, 2015.
[7] S.Y. Kim, H.S. Song and K. Nam, "Idling port isolation control of three-port bidirectional converter for EVs." *IEEE Transactions on Power Electronics.*, 27.5 (2012): 2495-2506.
[8] P. Sabine, M. Perrin, and A. Jossen. "Methods for state-of-charge determination and their applications." *Journal of power sources.*, 96.1 (2001): 113-120.